AIP | Journal of Applied Physics

Suppression of spatial hole burning and pulse stabilization for actively modelocked quantum cascade lasers using quantum coherent absorption

S. S. Shimu, A. Docherty, M. A. Talukder, and C. R. Menyuk

Citation: J. Appl. Phys. **113**, 053106 (2013); doi: 10.1063/1.4790145
View online: http://dx.doi.org/10.1063/1.4790145
View Table of Contents: http://jap.aip.org/resource/1/JAPIAU/v113/i5
Published by the American Institute of Physics.

JOURNAL OF APPLIED PHYSICS **113**, 053106 (2013)

Suppression of spatial hole burning and pulse stabilization for actively modelocked quantum cascade lasers using quantum coherent absorption

S. S. Shimu,[1,a)] A. Docherty,[1] M. A. Talukder,[1,2] and C. R. Menyuk[1]
[1]*Department of Computer Science and Electrical Engineering, University of Maryland Baltimore County, 1000 Hilltop Circle, Baltimore, Maryland 21250, USA*
[2]*Department of Electrical and Electronic Engineering, Bangladesh University of Engineering and Technology, Dhaka 1000, Bangladesh*

(Received 4 September 2012; accepted 16 January 2013; published online 5 February 2013)

We theoretically study of an actively modelocked quantum cascade laser in which we incorporate quantum coherent absorption by interleaving quantum coherent absorbing periods with gain periods. We show that this absorption suppresses the spatial hole burning that is responsible for pulse instability. As a consequence, the laser produces a stable train of single-peak soliton-like pulses with pulse durations less than 1.25 ps over a broad range of pump powers. We also show that the laser self-starts from initial quantum noise. © *2013 American Institute of Physics*. [http://dx.doi.org/10.1063/1.4790145]

I. INTRODUCTION

High-power mid-infrared stable short pulses have many important applications. These include remote sensing, high-speed free-space communications, pump-probe experiments, spectroscopy, and light detection and ranging (LIDAR). Active modelocking is an effective method to obtain short pulse train in the picosecond range. Capasso and co-workers have made significant advances in modelocking quantum cascade lasers (QCLs)[1–5] since the invention of QCLs in 1994.[6] Recently, mid-infrared short pulses on the order of few picoseconds have been experimentally observed in an actively modelocked QCL.[7] At pump powers between 1.0 and 1.1 times the continuous wave (CW) laser threshold, 8:1 autocorrelation traces were observed, leading the authors to conclude that stable pulses had been produced. However, theoretical studies investigating active modelocking in QCLs found that while pulses exist, they never reach a stationary state due to spatial hole burning (SHB).[8] Instead, the pulses evolve slowly, and have a complex multi-peak structure that is continuously changing. This slow evolution is consistent with 8:1 autocorrelation traces, but it implies that the pulses are not truly stable; they are at best quasi-stable. At pump powers above 1.1 times the CW laser threshold, 8:1 autocorrelation traces are no longer observed, and pulses are unquestionably unstable. The stability of actively modelocked pulses in QCLs is limited by SHB in the cavity. In most QCLs, the gain recovery time (T_1) and the diffusion time (T_d) are shorter than the round trip time (T_{rt}). When either $T_1 \ll T_{\mathrm{rt}}$ or $T_d < T_{\mathrm{rt}}$, SHB leads to the generation of waves that ultimately cause pulse breakup and chaos.

In Refs. 9–12, it has been shown theoretically that QCLs can be passively modelocked using the self-induced transparency (SIT) effect. SIT is a phenomenon in which a short pulse of coherent light above a critical input energy and a given pulse duration τ that is short compared to the coherence time T_2 of the medium can pass through an optically resonant medium as though it were transparent. When the pulse energy is below a critical energy, the pulse damps. In a typical QCL, we find $T_2 \ll T_1 \ll T_{\mathrm{rt}}$,[12,13] while the value of T_2 can be as large as 200 fs, which makes the QCL suitable to obtain SIT modelocking. However, SIT-modelocked QCLs do not self-start.

In this work, we theoretically study an actively modelocked QCL in which we add quantum coherent absorption by interleaving absorbing periods with gain periods. We show that the QCL self-starts from initial quantum noise and produces a stable train of single-peaked soliton-like modelocked pulses with pump powers that go up to at least twice the CW laser threshold. We determine the stability range of modelocked pulses for different pump powers and the effect of initial quantum noise on pulse formation.

II. MODELING OF QCL DYNAMICS

We have modeled an actively modelocked QCL similar to the device of Wang *et al.*,[7] but in which quantum coherent absorption may be added. This laser only has gain periods, and a detailed design for these gain periods is given in Ref. 7, but we do not use those designs here. Our modeling is based on solving the Maxwell-Bloch equations[5,8–12] for which the detailed band structure is not needed. The laser cavity is divided into two electrically isolated sections—a short section (0.24 mm) and a long section (2.36 mm). These lengths are same as in Ref. 8. Both sections are continuously pumped with the same DC pump current. Active modelocking is achieved by modulating the pump current in the short section with a modulation frequency equal to the cavity round-trip frequency. Hence, the inhomogeneous gain broadening due to inhomogeneous gain saturation is suppressed as the pulse remains under the gain peak of the Gaussian gain profile. Figure 1 shows a schematic illustration of the device structure. The QCL cavity is designed by interleaving gain and absorbing periods in which the dipole moment of the

a)Electronic mail: samia2@umbc.edu.

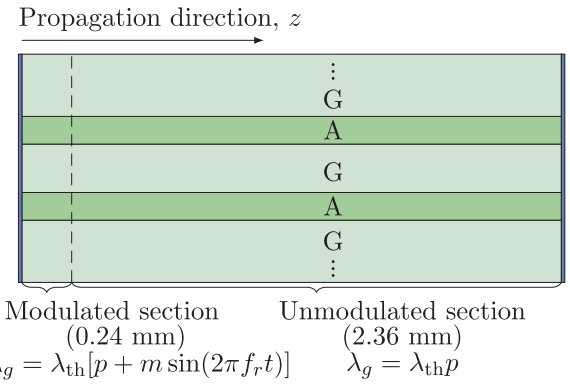

FIG. 1. Schematic illustration of an actively modelocked QCL with interleaved gain and absorbing periods. The labels G and A indicate gain and absorbing periods, respectively, and λ_g denotes the pumping strength.

absorbing periods d_a is approximately twice the dipole moment of the gain periods d_g, and the gain and absorbing periods are in resonance. We have previously published detailed layer designs that achieve these conditions.[9,10]

We used an open two-level system to model the QCL dynamics.[8] If both quantum coherent gain and absorbing periods are present, the electric field will interact with both period types simultaneously, as long as the spacing between the periods is small compared to the wavelength of the light, and will respond to the average properties of the periods. We may use the bi-directional Maxwell-Bloch equations,

$$\frac{n}{c}\frac{\partial E_\pm}{\partial t} = \mp\frac{\partial E_\pm}{\partial z} - i\frac{N_g\Gamma_g d_g k}{\epsilon_0 n^2}\eta_{g\pm} - i\frac{N_a\Gamma_a d_a k}{\epsilon_0 n^2}\eta_{a\pm} - lE_\pm, \tag{1a}$$

$$\frac{\partial \eta_{g\pm}}{\partial t} = \frac{id_g}{2\hbar}(\Delta_{0g}E_\pm + \Delta_{2g}^{\mp}E_\mp) - \frac{\eta_{g\pm}}{T_{2g}}, \tag{1b}$$

$$\frac{\partial \eta_{a\pm}}{\partial t} = \frac{id_a}{2\hbar}(\Delta_{0a}E_\pm + \Delta_{2a}^{\mp}E_\mp) - \frac{\eta_{a\pm}}{T_{2a}}, \tag{1c}$$

$$\frac{\partial \Delta_{0g}}{\partial t} = \lambda_g + \frac{i}{\hbar}d_g(E_+^*\eta_{g+} + E_-^*\eta_{g-} - \text{c.c.}) - \frac{\Delta_{0g}}{T_{1g}}, \tag{1d}$$

$$\frac{\partial \Delta_{0a}}{\partial t} = \lambda_a + \frac{i}{\hbar}d_a(E_+^*\eta_{a+} + E_-^*\eta_{a-} - \text{c.c.}) - \frac{\Delta_{0a}}{T_{1a}}, \tag{1e}$$

$$\frac{\partial \Delta_{2g}^{\pm}}{\partial t} = i\frac{d_g}{\hbar}(E_\pm^*\eta_{g\mp} - E_\mp\eta_{g\pm}^*) - \left(\frac{1}{T_{1g}} + 4k^2D\right)\Delta_{2g}^{\pm}, \tag{1f}$$

$$\frac{\partial \Delta_{2a}^{\pm}}{\partial t} = i\frac{d_a}{\hbar}(E_\pm^*\eta_{a\mp} - E_\mp\eta_{a\pm}^*) - \left(\frac{1}{T_{1a}} + 4k^2D\right)\Delta_{2a}^{\pm}, \tag{1g}$$

where E_x denotes the envelope of the electric field, η_x denotes the dielectric polarization, Δ_{0x} denotes the average population inversion, and Δ_{2x} denotes the inversion grating. The quantities with a $+(-)$ subscript or superscript represent fields that are propagating in the positive (negative) z direction, and the subscripts g and a represent gain and absorption, respectively. The parameters E_x, η_x, Δ_{0x}, and Δ_{2x} are assumed to vary slowly with respect to space z and time t. The parameter n denotes the index of refraction, c denotes the speed of light, ϵ_0 denotes the vacuum permittivity, $\hbar$ denotes the Planck's constant, N_x denotes the electron density in the active region, Γ_x denotes the overlap factor between the laser mode and the active region, T_{1x} denotes the gain recovery time, T_{2x} denotes the dephasing time, l denotes the linear cavity (not quantum coherent) loss per unit length not including mirror losses, λ_x denotes the pump parameter, D denotes the diffusion coefficient, d_x denotes the dipole matrix element of the laser transition, and k denotes the wave number associated with the optical resonance frequency. We may write $k \equiv \omega n/c$, where ω denotes the angular frequency of the electric field.

In the short section of the cavity, the pump parameter λ_g, which corresponds to λ in Ref. 8, is given by

$$\lambda_g = \lambda_{th}[p + m\sin(2\pi f_r t)], \tag{2}$$

where λ_{th} denotes the threshold pump parameter, p denotes the ratio of the pump power to the threshold pump power, m denotes the modulation depth, and f_r denotes the cavity round-trip frequency. In the long section of the cavity, in which the pumping is not modulated, we have $\lambda_g = \lambda_{th}p$. The threshold λ_{th} is given by $\lambda_{th} = gl_t/T_{1g}T_{2g}$, where g is the gain per unit length, and l_t is the total cavity loss. This loss includes both material and facet losses and is given by

$$l_t = l + \frac{1}{2L_c}\ln\left(\frac{1}{r_1}\right) + \frac{1}{2L_c}\ln\left(\frac{1}{r_2}\right), \tag{3}$$

where r_1 and r_2 denote the reflectivity of the two facets, and L_c denotes the length of the laser cavity. We now find that λ_a in Eq. (1e) is given by $\lambda_a = \lambda_g(a/g)(T_{1g}T_{2g}/T_{1a}T_{2a})$, where a is the quantum coherent absorption per unit length. If $T_{1a} = T_{1g}$ and $T_{2a} = T_{2g}$, as will be the case in all our simulations, then we find that $\lambda_a/\lambda_g = a/g$ in both sections of the cavity.

To suppress the formation of continuous waves, the gain must be below the CW laser threshold.[10] If we set $E_+ = E_- \equiv E$ at steady state, the CW steady-state polarizations in the gain and absorbing periods become

$$\eta_{g\pm} = \frac{id_gT_{2g}}{2\hbar}(\Delta_{0g}E + \Delta_{2g}^{\mp}E) \quad \text{and}$$
$$\eta_{a\pm} = \frac{id_aT_{2a}}{2\hbar}(\Delta_{0a}E + \Delta_{2a}^{\mp}E). \tag{4}$$

After substituting $\eta_{g\pm}$, $\eta_{a\pm}$, and the total loss into Eq. (1a) and noting that the derivative of the CW electric field vanishes, we obtain

$$\frac{N_g\Gamma_g d_g^2 kT_{2g}}{2\epsilon_0 n^2\hbar}(\Delta_{0g}E + \Delta_{2g}^{\mp}E) + \frac{N_a\Gamma_a d_a^2 kT_{2a}}{2\epsilon_0 n^2\hbar} \times (\Delta_{0a}E + \Delta_{2a}^{\mp}E) - l_tE = 0. \tag{5}$$

TABLE I Simulation Parameters

Parameter	Symbol	Value
Gain recovery time	T_1	50 ps
Dephasing time	T_2	50 fs
Diffusion time	T_d	5 ps
Linear cavity loss	l	10 cm^{-1}
Cavity length	L_c	2.6 mm
Facet reflectivity	r_1, r_2	0.53
Modulation depth	m	5
Index of refraction	n	3.2

At steady state, we also find $\Delta_{0g} = \lambda_g T_{1g}$ and $\Delta_{0a} = \lambda_a T_{1a}$ for the gain and absorbing periods, respectively. Also, at threshold, there is no inversion grating, so that Eq. (5) becomes

$$\frac{N_g \Gamma_g d_g^2 k T_{2g}}{2\epsilon_0 n^2 \hbar} \lambda_g T_{1g} + \frac{N_a \Gamma_a d_a^2 k T_{2a}}{2\epsilon_0 n^2 \hbar} \lambda_a T_{1a} - l_t = 0, \quad (6)$$

which can be written as $g\lambda_g T_{1g} + a\lambda_a T_{1a} - l_t = 0$ or,

$$\bar{g} - \bar{a} - 1 = 0, \quad (7)$$

where,

$$g = \frac{N_g \Gamma_g d_g^2 k T_{2g}}{2\epsilon_0 n^2 \hbar}, \qquad a = \frac{N_a \Gamma_a d_a^2 k T_{2a}}{2\epsilon_0 n^2 \hbar},$$
$$\bar{g} = g\lambda_g T_{1g}/l_t, \qquad \bar{a} = -a\lambda_a T_{1a}/l_t. \quad (8)$$

Here, the parameters g and a correspond, respectively, to the gain and quantum coherent absorption per unit length, whereas $\bar{g}$ and $\bar{a}$ correspond to the gain and quantum coherent absorption with respect to the usual incoherent cavity attenuation, respectively.

We used a bi-directional second-order finite-difference method to solve Eq. (1). The parameter values used in our simulation are given in Table I. We used the same sets of parameter values for the gain periods as in Ref. 8, so that we can compare our results to theirs. For the absorbing periods, we assumed that the dipole moment is twice as large as that in the gain periods, so that $d_a = 2d_g$. We also assumed that the dephasing time and the gain recovery time of the absorbing periods are equal to those in the gain periods, so that $T_{2a} = T_{2g} \equiv T_2$ and $T_{1a} = T_{1g} \equiv T_1$. We assumed that the diffusion time $T_d = 1/4k^2D = 5$ ps. Following Gkortsas *et al.*,8] we will use p, the power relative to the threshold in the absence of quantum coherent absorption, to parameterize the gain. For the parameters in Table I, we find that $p = 1$ corresponds to $\bar{g} = 1.244$.

III. SIMULATION RESULTS

We have carried out simulations with and without quantum coherent absorption. In our first set of simulations, the laser is pumped at 1.61 times, the threshold power that is required to initiate lasing in a QCL without absorbing periods. When quantum coherent absorption is not present, we set $\bar{a} = 0$. When it is present, we set $\bar{a} = 0.801$, which corresponds to an intermediate value in the range over which we observed stability. We note that the round trip frequency depends on the pulse intensity and must be determined computationally. Figure 2 shows the normalized intensity and population inversion as a function of position inside the laser cavity. The total inversion Δ is a combination of the average inversion Δ_0 and the inversion grating $\Delta_2^{\pm}$ and is given by

$$\Delta = \Delta_0 + \Delta_2^{+}\exp(2ikz) + \Delta_2^{-}\exp(-2ikz). \quad (9)$$

Without quantum coherent absorption, the interference of the two counter-propagating waves produces a standing wave pattern in the cavity, which introduces inhomogeneous gain saturation of the laser medium, i.e., SHB. Due to SHB, more modes start lasing, and the intensity fluctuates along the cavity length, as shown in Fig. 2(a). On the contrary, when quantum coherent absorption periods are interleaved with the gain periods, the SHB is suppressed, and we observe a stable pulse with a single-peaked soliton-like pulse shape inside the cavity as shown in Fig. 2(b).

Figure 3 shows the normalized intensity of the output pulses for different DC pump powers after 500 round trips. The intensity is normalized with respect to $(\hbar/d_g)^2$. We set $\bar{a} = 0$ when quantum coherent absorption is absent, and we choose values of $\bar{a}$ that are appropriate to obtain stable

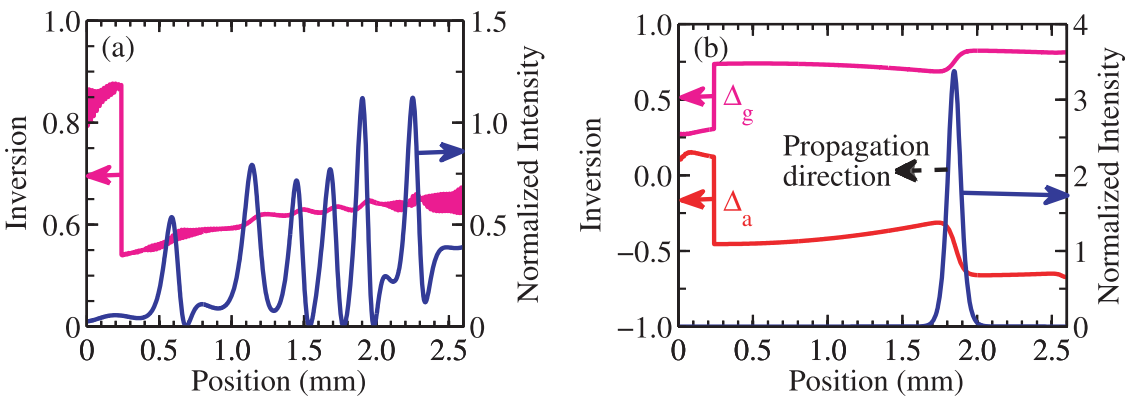

FIG. 2. Normalized intensity (blue line) and total inversion as a function of position inside the laser cavity after 600 round trips with $p = 1.61$, $\bar{g} = 2.0$; (a) without quantum coherent absorption, i.e., $\bar{a} = 0$, and (b) with quantum coherent absorption, i.e., $\bar{a} = 0.801$. We note the complete suppression of SHB in (b).

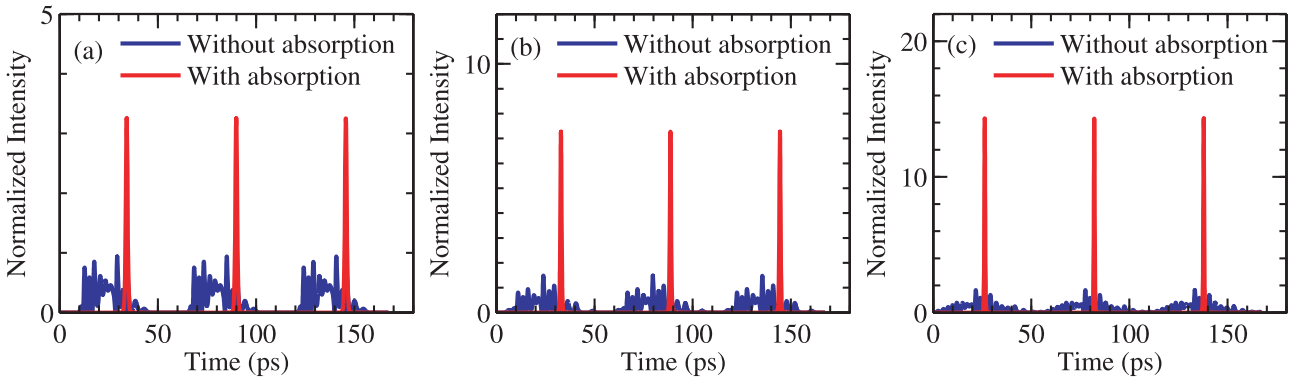

FIG. 3. The normalized output pulse intensity. Unstable multi-peak pulses are observed when there is no quantum coherent absorption (blue line). When quantum coherent absorption is added, stable single-peak pulses are found to exist (red line). We have (a) $p = 1.61$, $\bar{g} = 2.0, \bar{a} = 0.801$; (b) $p = 1.8$, $\bar{g} = 2.239, \bar{a} = 1.019$; (c) $p = 2.0$, $\bar{g} = 2.488, \bar{a} = 1.244$.

single-peak pulses when it is present. When quantum coherent absorption is absent, the pulse is not stable at any pump power. The pulse shape is complex with multiple peaks and never reaches a steady state (blue line). This result is consistent with that of Gkortsas *et al.*[8] On the other hand, we obtained a stable train of single-peak output pulses with a fixed repetition rate when quantum coherent absorption is present (red line). For $p = 1.61$, we obtain output pulses with a full-width-at-half-maximum (FWHM) pulse duration of 1.25 ps. When we increase the pump power, the intensity of the peak of the output pulse increases and the pulse duration decreases. We obtain stable FWHM pulse durations of 0.86 ps and 0.63 ps for $p = 1.8$ and $p = 2.0$, respectively. Thus, we are predicting that it is possible to obtain sub-ps pulses in this actively modelocked system. That is consistent with the work by Dudley *et al.*[14] showing that the SIT effect can be used to shape the duration of modelocked pulses.

In Fig. 4, we show the stability range of output pulses for different pump powers. We obtain stable single-peaked output pulses when gain and absorption are set between the upper (blue line) and lower (red line) boundaries. The pulses become unstable for any combination of gain and absorption below the lower boundary due to SHB. In particular, pulses are always unstable unless quantum coherent absorption is present. For any values above the upper boundary, the pulse attenuates exponentially. The duration of the stable pulse can be controlled by varying the gain and absorption per unit length. Figure 4 shows that the stable range of quantum coherent absorption values varies by about $\pm 2\%$ around its optimum value when $p = 1.61$ and by about $\pm 6\%$ when $p = 2.0$ and the stability range of the output pulses increases at high pump powers. We have also found that as T_2 increases, so does the stable output pulse range.

Figure 5 shows the normalized peak pulse intensity of the laser output over time when the pulses is grown from different initial noise levels. With quantum coherent absorption, the pulse intensity grows from initial quantum (spontaneous emission) noise and reaches a stable stationary state. We calculate this initial quantum noise assuming that there is one noise photon per temporal mode and that the laser is operating in a single transverse mode with an effective area $A_{\text{eff}} = 2.56 \times 10^{-4}\,\text{mm}^2$. We normalized the intensity with respect to $(\hbar/d_g)^2$. The normalized initial quantum noise intensity is 3×10^{-8}. Since the actual noise level will be higher in any real device due to technical noise, we investigated the behavior as we increased the initial noise level over 6 decades. As observed in Fig 5, the only effect is to halve the time at which the pulse grows to a visible amplitude.

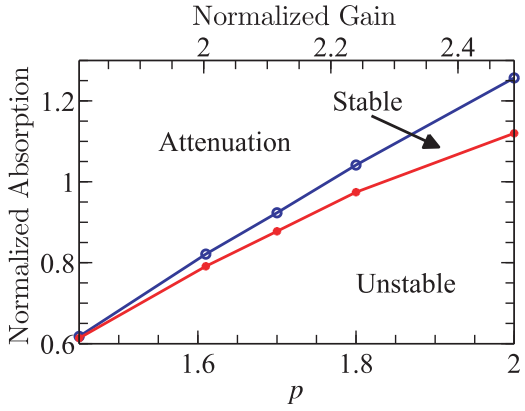

FIG. 4. Stability range of pulses for different combinations of gain and quantum coherent absorption.

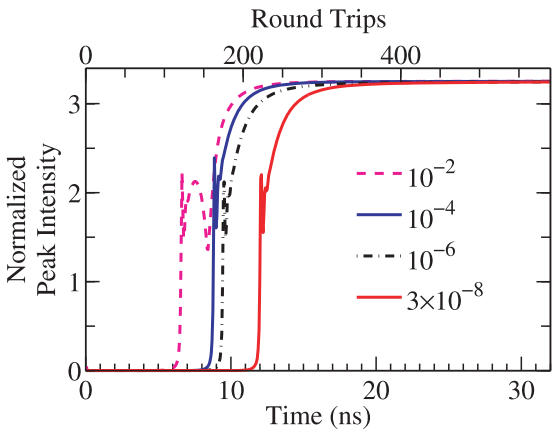

FIG. 5. Normalized peak pulse intensity starting from different noise levels.

IV. DISCUSSION AND CONCLUSION

In conclusion, we show that it is possible to suppress SHB in an actively modelocked QCL by adding quantum coherent absorption. It might seem surprising at first that a quantum dephasing time (T_2) as short as 50 fs is sufficient to suppress SHB. To understand this suppression, we note that the oscillation period associated with the SHB is given by $T_{SHB} = 1/2f = \pi n/kc \simeq 10\,\text{fs}$. As long as $T_2 > T_{SHB}$, as is the case here, SHB should be suppressed. We have not investigated the transition from the limit $T_2 > T_{SHB}$ to the limit $T_2 < T_{SHB}$ in detail since the slowly varying envelope approximation is no longer valid, but we have verified that when $T_2 \ll T_{SHB}$, so that the time derivatives in Eqs. (1b) and (1c) can be ignored, the SHB is no longer suppressed. The suppression of SHB allows active modelocking to generate stable single-peak soliton-like pulses over a broad range of pump powers. The stability range of the output pulses increases as the pump power increases. We also show that the laser self-starts from initial quantum noise or higher noise levels.

ACKNOWLEDGMENTS

This research work was supported by the National Science Foundation under the auspices of the MIRTHE Engineering Research Center.

[1]R. Paiella, F. Capasso, C. Gmachl, D. L. Sivco, J. N. Baillargeon, A. L. Hutchinson, A. Y. Cho, and H. C. Liu, Science **290**, 1739–1742 (2000).
[2]R. Paiella, F. Capasso, C. Gmachl, H. Y. Hwang, D. L. Sivco, A. L. Hutchinson, A. Y. Cho, and H. C. Liu, Appl. Phys. Lett. **77**, 169–171 (2000).
[3]A. Soibel, F. Capasso, C. Gmachl, M. L. Peabody, A. M. Sergent, R. Paiella, D. L. Sivco, A. Y. Cho, and H. C. Liu, IEEE J. Quantum Electron. **40**, 197–204 (2004).
[4]A. Soibel, F. Capasso, C. Gmachl, M. L. Peabody, A. M. Sergent, R. Paiella, H. Y. Hwang, D. L. Sivco, A. Y. Cho, H. C. Liu, C. Jirauschek, and F. X. Kärtner, IEEE J. Quantum Electron. **40**, 844–851 (2004).
[5]C. Y. Wang, L. Diehl, A. Gordon, C. Jirauschek, F. X. Kärtner, A. Belyanin, D. Bour, S. Corzine, G. Höfler, M. Troccoli, J. Faist, and F. Capasso, Phys. Rev. A **75**, 031802(R) (2007).
[6]J. Faist, F. Capasso, D. L. Sivco, C. Sirtori, A. L. Hutchinson, and A. Y. Cho, Science **264**, 553–556 (1994).
[7]C. Y. Wang, L. Kuznetsova, V. M. Gkortsas, L. Diehl, F. X. Kärtner, M. A. Belkin, A. Belyanin, X. Li, D. Ham, H. Schneider, P. Grant, C. Y. Song, S. Haffouz, Z. R. Wasilewski, H. C. Liu, and F. Capasso, Opt. Express **17**, 12929–12943 (2009).
[8]V. M. Gkortsas, C. Wang, L. Kuznetsova, L. Diehl, A. Gordon, C. Jirauschek, M. A. Belkin, A. Belyanin, F. Capasso, and F. X. Kärtner, Opt. Express **18**, 13616–13630 (2010).
[9]C. R. Menyuk and M. A. Talukder, Phys. Rev. Lett. **102**, 023903 (2009).
[10]M. A. Talukder and C. R. Menyuk, Appl. Phys. Lett. **95**, 071109 (2009).
[11]M. A. Talukder and C. R. Menyuk, Phys. Rev. A **79**, 063841 (2009).
[12]M. A. Talukder, Ph.D. dissertation, University of Maryland Baltimore County, 2010.
[13]C. Sirtori and R. Teissier, "Quantum cascade lasers: overview of basic principles of operation and state of the art," in *Intersubband Transitions in Quantum Structure*, edited by R. Paiella, (McGraw-Hill, New York, 2006).
[14]M. J. Dudley, J. D. Harvey, and R. Leonhardt, J. Opt. Soc. **10**, 840–851 (1993).